Observations of two seasons of sintering in a mountain snowpack

Edward H. Bair[1,*], Jeff Dozier[1], Robert E. Davis[2], Thomas U. Kaempfer[2],
Michael T. Colee[1], Randall Mielke[1], and Jane R. Blackford[3]
[1] Bren School of Environmental Science & Management, University of California,
Santa Barbara CA U.S.A.
[2] US Army Cold Regions Research and Engineering Laboratory, Hanover NH U.S.A.
[3] Centre for Materials Science and Engineering, University of Edinburgh, Scotland

ABSTRACT: We present results from an ongoing two-year study at Mammoth Mountain, California. We track multiple layers, starting at a variety of initial conditions and subjected to different temperature gradients, from deposition to melt at two different sites. We examine samples with optical microscopy under cross-polarized light, with low-temperature scanning electron microscopy, and with an x-ray spectrometer. The neck ratio (bond diameter to grain radius) quickly approaches a value of 0.5-0.6. Density increases linearly throughout the season with grain diameter, but inter-grain distance, measured from grain centre to grain centre, also increases. An explanation for this counterintuitive behaviour is that coarsening is the rate-limiting step. Densification, caused by sintering, is re-initiated by coarsening. We observe impurities typical of Sierra snow with no difference in spatial distribution, measured 6 times in a season. As a case study, we examine sintering changes in a weak layer that was responsible for destructive avalanches in December 2008, including one that severely injured a Mammoth patroller.

KEYWORDS: sintering, avalanche, microscopy.

1 INTRODUCTION

Snow is constantly driven by thermodynamic forces to minimize free energy. In the atmosphere, crystals grow kinetically into different forms— including dendrites, rods, columns, and needles—as they pass through different conditions of supersaturation and temperature. Small changes in local environment cause different forms and sizes to be deposited during storms. Once snow falls, packing arrangements cause neighbouring crystals to have different radii of curvature.

Natural snow usually has micro-scale temperature gradients, which enhance vapour flux and probably increase sintering rate. New snow crystals begin to sinter within seconds of contact (Gubler, 1982). Freezing of a thin liquid layer is the likely mechanism (Szabo and Schneebeli, 2007). At the ice surface, hydrogen and oxygen atoms vibrate with more amplitude than those in the interior. The interaction between the surface and interior atoms creates melt at the surface (Ikeda-Fukazawa and Kawamura, 2004).

Studies thus far have examined snow grown in laboratories (Kingery, 1960; Kuroiwa, 1961; Hobbs and Mason, 1964), taken at a single time from the natural snowpack (Adams et al., 2001; Rosenthal et al., 2007), or sampled from natural snow and metamorphosed in the laboratory (Schneebeli and Sokratov, 2004). We present a time series of observations of seasonal snow and relate them to previous work.

* Corresponding author address: Edward H. Bair, Bren School of Environmental Science & Management, University of California, Santa Barbara CA 93106-5131, USA; tel 703-217-7214, email nbair@bren.ucsb.edu.

2 METHODS

2.1 *In situ*

We collected samples at two sites on Mammoth Mountain, California, during the winters of 2007-08 and 2008-09 (Table 1). We began collection shortly after the first significant snowfall of the season, in November or December, and ended collection when the pack became isothermal, sometime in April. On average, we collected samples every two weeks, with intervals ranging from five weeks to less than 24 hr. We collected samples on 6 dates in 2007-08 and 14 dates in 2008-09. Usually, we dug a full profile pit and measured densities and temperatures every 10 cm. Temperature gradients were assumed to be linear under 10cm. To assure that we sampled the same layers each time, we used depth of the layer from the previous measurement, hand hardness, and the presence of ice lenses and crusts to guide us.

Table 1. Layers sampled at Mammoth Mountain. Identifiers correspond to layers and locations in figures.

ID	*Description*	*Sampling Site*
(a)	2007-08 basal layer	Mid-Mountain
(b)	2008-09 layer 2	Mid-Mountain
(c)	2008-09 top layer	Mid-Mountain
(d)	2007-08 basal layer	Ski Patrol Plot

2.2 *Storage and Transport*

We placed samples in fist-sized steel containers, transported them in a liquid N_2 dry ship-

per from Mammoth to UC Santa Barbara, where we stored them at –152°C. We believe these low temperatures inhibit structural changes. Erbe et al. (2003) used these techniques to store snow for as long as 3 years without significant changes.

2.3 *Cross-polarized microscopy*

We brought samples from the refrigerator to a cold room at –5°C and began examination within 15 minutes, allowing them to warm enough to be handled with metal forceps. We placed samples on a glass dish with a ruler for scale and imaged them under cross-polarized light using a macroscope outfitted with digital camera.

2.4 *Stereology*

Rather than preparing thin-sections (Bader et al., 1939; Kinosita and Wakahama, 1960), serial sections (de Quervain, 1973; Davis and Dozier, 1989), or microtomogaphs (Schneebeli and Sokratov, 2004; Kaempfer and Schneebeli, 2007), we used cross polarizing filters to delineate grain orientation for disaggregated snow samples. We tracked the mean bond diameter *X* and the mean grain diameter *D*, taken as the mean of the major and minor axis length (Figure 1). *X* and *D* were computed by averaging ~20 disaggregated crystals. Furthermore, we measured inter-grain distance, being the centre to centre distance between adjacent crystals.

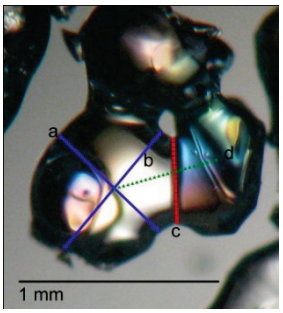

Figure 1. Stereological measurements for layer (a) at day 126.

a. minor axis
b. major axis
c. bond diameter
d. inter-grain distance

2.5 *Low temperature scanning electron microscopy*

See Rosenthal et al. (2007) for a description of our methods. A difference between our study and theirs was that chemical impurities were examined using an EDAX energy dispersive x-ray spectrometer (EDS) instead of the Princeton Gamma Tech EDS.

3 RESULTS AND DISCUSSION

3.1 *In situ*

Figure 2 shows that most of the time, density grows linearly at similar rates and temperature gradients are small. Exceptions occur immediately after deposition, when we see rapid density increases and steep temperature gradients. Neck ratio growth for the layer examined daily (Figure 3c) and abrupt decrease in densification rate after the first 3 days (Figure 2c) suggest a change in the process controlling densification.

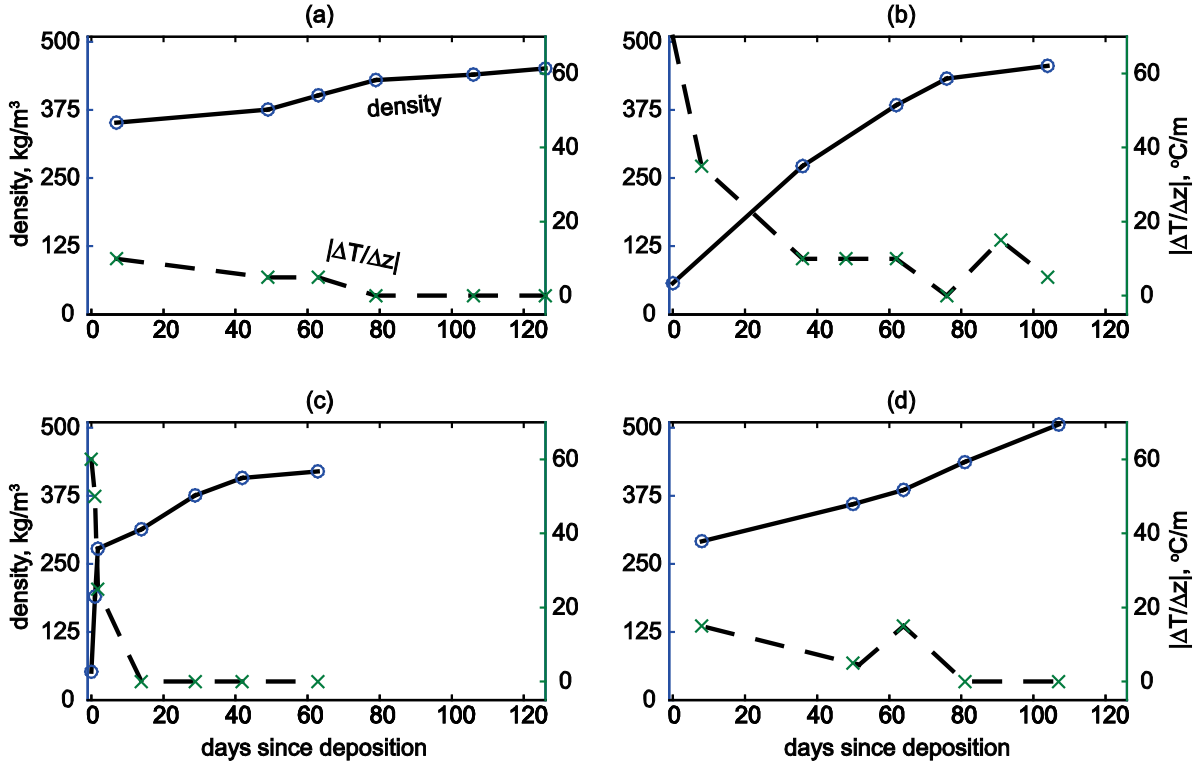

Figure 2. Density (left axes) and temperature gradients (right axes). The letters correspond to the layers and locations identified in Table 1.

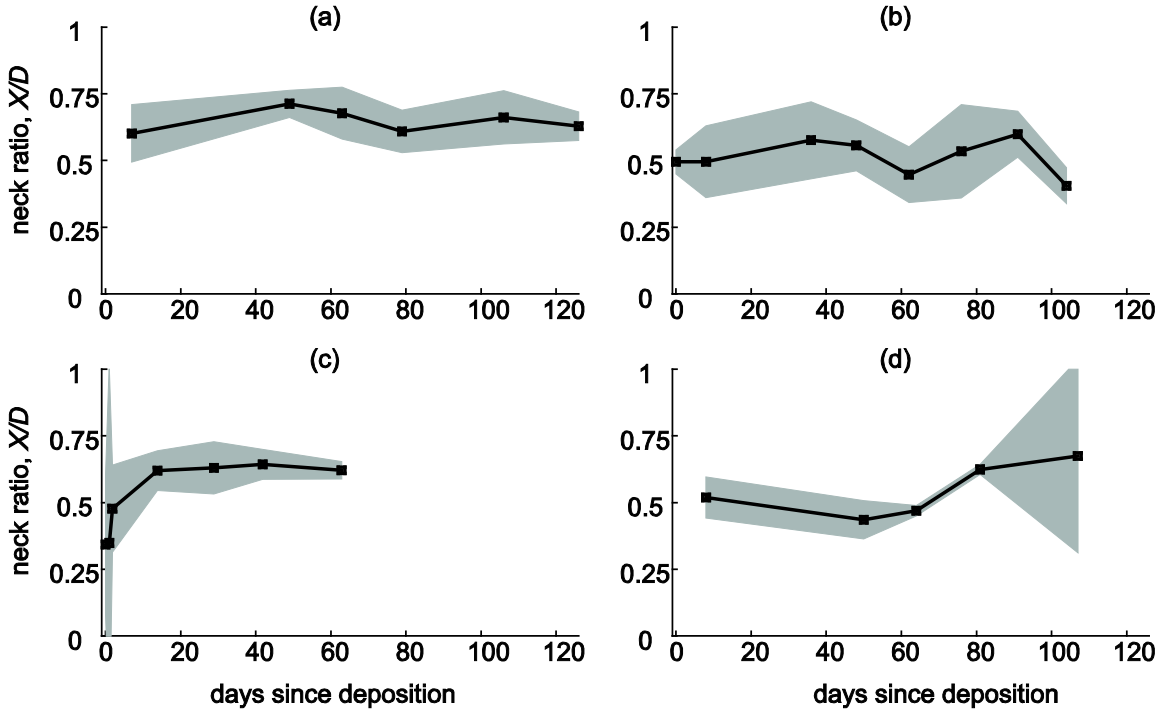

Figure 3. Mean neck ratios and standard deviations. Ordinates are the ratio of bond diameter *X* to grain diameter *D.* The letters correspond to the layers and locations identified in Table 1.

Temperature gradients are small most of the time, with the exception of the first two samples for Layers (b) and (c).

3.2 Cross polarized microscopy

Neck ratios do not grow according to a power law but rapidly increase to around 0.5-0.6 within a few days after deposition (Figure 3). In Layer (c), there is growth in the neck ratio during the first four observations (Figure 3c), but this layer experienced moderate temperature gradients during the first three observations (Figure 2c). During this time, kinetic growth was probably dominant because of moderate vapour fluxes. The rapid increase in density during the first 3 days (Figure 2c) also suggests bulk transport mechanisms.

Layer (b) was particularly interesting, as large facets and depth hoar crystals grew during the first 7 days, but the neck ratio remained constant as it did for the two basal Layers (a) and (d), which were composed of rounded forms. We conclude that crystal form alone does not affect the sintering rate.

Neck ratios appear constant with time, with the exception of one layer (Figure 3c), which was the only layer examined daily for the first 3 observations. This layer shows growth in its neck ratio from 0.38 to 0.60 during the first 10 days.

Although we observed constant neck ratios, grains grew. Grain radius increases linearly with density, bond diameter, and inter-grain distance (Figure 4), measured from grain centres. The shaded areas in Figure 3 are the result of large differences in radii of curvature and limited sample size. Persistent differences in radii of curvature also suggest that coarsening is constantly occurring.

Coarsening, as a rate-limiting step for sintering, is a likely explanation for the increase in density, grain diameter, bond diameter, and inter-grain distance. We use a theoretical framework (Lange and Kellett, 1989) to suggest the following order of events:

- Grains of different radii are deposited. High sensitivity to local environment as the grain travels through the atmosphere causes adjacent grains to have different radii of curvature.
- Adjacent grains with sufficient difference in radii of curvature will sinter to minimize free energy. The condition for sintering is R_1/R_2, $\leq R_c$ where R_1 and R_2 are radii of curvature, and R_c is the critical value. Sintering continues until the grain ratio is above the critical value.
- Sintering can only be re-initiated once there is sufficient difference in the radii of curvature. For this to happen, the smaller particle must disappear completely due to coarsening.
- This process repeats until maximum density (~500kg/m^3), at which point free energy for the system is minimized.

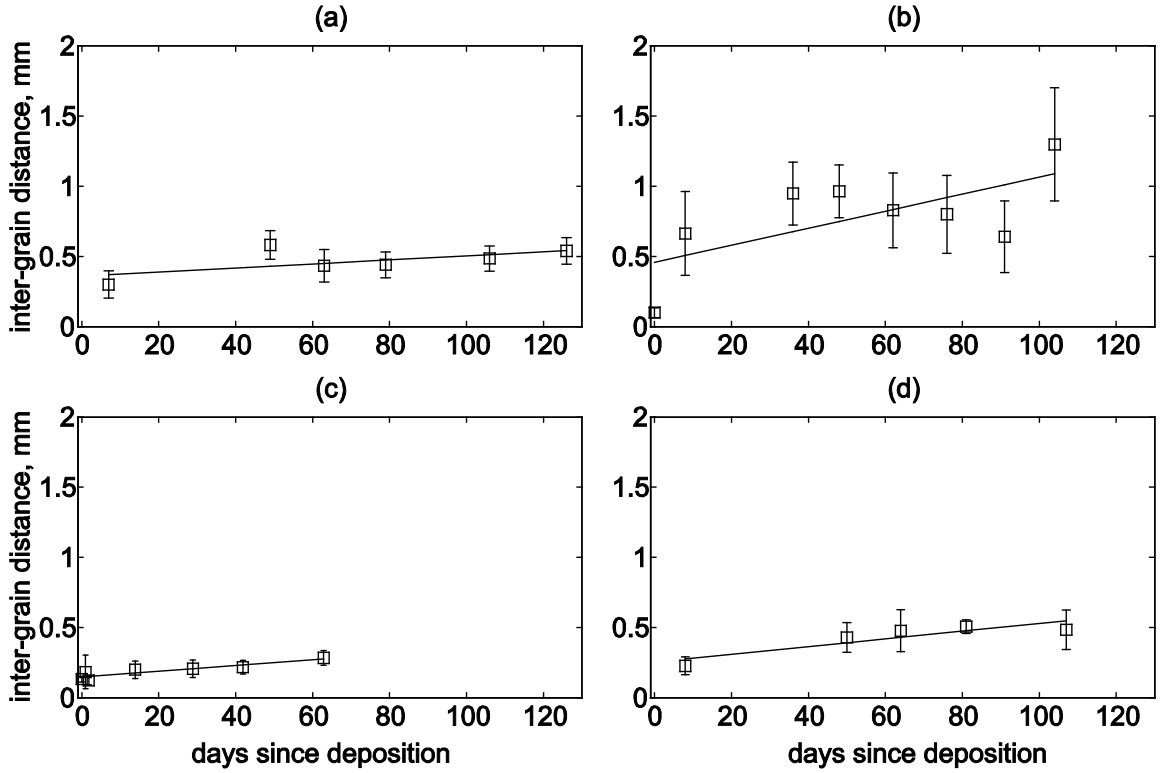

Figure 4. Mean inter-grain distance *L* and standard deviation vs time *t*. The letters correspond to the layers and locations identified in Table 1.

3.3 Low temperature scanning electron microscopy

Other studies have found that soluble impurities migrate towards grain boundaries (Adams et al., 2001; Blackford, 2007; Rosenthal et al., 2007). If you consider that grain surfaces can also be boundaries, our findings support this. We examined impurity concentrations at 6 dates, from day 7-126, for Layer (a) by taking EDS point samples at bonds and at grain surfaces. We found impurities typical of Sierra snow, with little difference in spatial distribution between bond and grain surfaces.

We also used the SEM to determine the dihedral angle at grain boundaries. Mostly, it is near the predicted equilibrium value of 145° (Colbeck, 1998; Blackford, 2007). This suggests that dihedral angle growth occurred prior to the first 7 days, when the first sample was collected. Other studies have confirmed that dihedral angle evolution proceeds rapidly. Blackford et al. (2007) found dihedral angles of approximately 120° after 1 hr of sintering ice spheres doped with small quantities of NaCl at –8°C.

4 CASE STUDY: DEEP INSTABILITIES THAT FAILED ON LAYER (B) DURING 2008-09

All avalanches that failed on Layer (b), except one, occurred within 12 days of deposition, suggesting that sintering times for the pack to gain enough strength to prevent deep instabilities are on that order. On day 2, an avalanche that likely failed on Layer (b), seriously injured a Mammoth patroller while ski-cutting for avalanche control. The avalanche fractured above the patroller and swept him into tightly spaced trees. There was one outlier, a class R4 that occurred on day 42, on a sheltered, north-facing pocket below a cliff band. The outlier suggests that steep isolated areas may take over 3x the amount of time to strengthen than what we observed on our flat study plot.

5 CONCLUSION

We find constant neck ratios, despite increasing grain and bond sizes. Combing this evidence with increasing inter-grain distance, we conclude that coarsening is the main cause and that it appears to limit the rate of sintering. The linear increase in density, present in all layers, shows that bulk transport must be occurring. These findings are supported by Kaempfer and Schneebeli (2007), who find similar results with isothermal snow stored in a laboratory at different temperatures. We find rapid increases in density, grain size, and some increase in neck ratio during the first three days for Layer (c), the only layer that we were able to examine daily. These increases show that rapid changes took place within the first 36 hr, but the presence of a moderate temperature gradient suggests that

kinetic growth occurred along with sintering. New snow is unlikely to be isothermal shortly after deposition; therefore, traditional sintering models cannot be applied.

Dihedral angles appear to be near the equilibrium value of 145°, independent of sample date. This suggests that growth in dihedral angle occurs soon after deposition. EDS results show no significant differences between point spectra taken on bond and grain surfaces.

We examined a weak layer that was responsible for deep instabilities during the winter of 2008-09. All avalanche activity occurred within 12 days of snow deposition, except for an isolated case. During the first 7 days, grain diameter and inter-grain distance increased rapidly and an unstable depth hoar layer formed. We suggest both measures are correlated with observed avalanche activity. The instability persisted for 12 days in most areas, but took up to 42 days to gain sufficient strength to prevent deep failures.

Acknowledgment: This research was funded by NSF Grant EAR-0537327. The first author is supported by a student fellowship from the U.S. Army Cold Regions Research and Engineering Laboratory.

6 REFERENCES

Adams, E. E., Miller, D. A., and Brown, R. (2001), Grain boundary ridge on sintered bonds between ice crystals, *Journal of Applied Physics*, 90(11): 5782-5785, doi: 10.1063/1.1410889.

Bader, H., Haefeli, R., Bucher, E., Neher, J., Eckel, O., and Thams, C. (1939), Snow and its metamorphism, SIPRE Translation 14, 313 pp.

Blackford, J. R. (2007), Sintering and microstructure of ice: A review, *Journal of Physics D: Applied Physics*, 40(21): R355-R385, doi: 10.1088/0022-3727/40/21/R02.

Blackford, J. R., Jeffree, C. E., Noake, D. F. J., and Marmo, B. A. (2007), Microstructural evolution in sintered ice particles containing NaCl observed by low-temperature scanning electron microscope, *Proceedings of the Institution of Mechanical Engineers, Part L: Journal of Materials: Design and Applications*, 221(3): 151-156, doi: 10.1243/14644207JMDA134.

Colbeck, S. C. (1998), Sintering in a dry snow cover, *Journal of Applied Physics*, 84(8): 4585-4589, doi: 10.1063/1.368684.

Davis, R. E., and Dozier, J. (1989), Stereological characterization of dry alpine snow for microwave remote sensing, *Advances in Space Research*, 9(1): 245-251, doi: 10.1016/0273-1177(89)90492-4.

de Quervain, M. (1973), Snow structure, heat and mass flux through snow. In: *The Role of Snow and Ice in Hydrology*, (Unesco / WMO / IAHS, Ed.), vol. 1, IAHS Publication 107, pp. 203-226.

Erbe, E. F., Rango, A., Foster, J., Josberger, E. G., Pooley, C., and Wergin, W. P. (2003), Collecting, shipping, storing, and imaging snow crystals and ice grains with low-temperature scanning electron microscopy, *Microscopy Research and Technique*, 62(1): 19-32, doi: 10.1002/jemt.10383.

Gubler, H. (1982), Strength of bonds between ice grains after short contact times, *Journal of Glaciology*, 28(100): 457-473.

Hobbs, P. V., and Mason, B. J. (1964), The sintering and adhesion of ice, *Philosophical Magazine*, 9: 181-196.

Ikeda-Fukazawa, T., and Kawamura, K. (2004), Molecular-dynamics studies of surface of ice Ih, *Journal of Chemical Physics*, 120: 1395-1401, doi: 10.1063/1.1634250.

Kaempfer, T. U., and Schneebeli, M. (2007), Observation of isothermal metamorphism of new snow and interpretation as a sintering process, *Journal of Geophysical Research*, 112: D24101, doi: 10.1029/2007JD009047.

Kingery, W. D. (1960), Regelation, surface diffusion, and ice sintering, *Journal of Applied Physics*, 31: 833-838.

Kinosita, S., and Wakahama, G. (1960), Thin sections of deposited snow made by the use of analine, Contribution 15:35-45, Institute of Low Temperature Science, Hokkaido University, Sapporo, Japan.

Kuroiwa, D. (1961), A study of ice sintering, *Tellus*, 13: 252-259.

Lange, F. F., and Kellett, B. (1989), Thermodynamics of densification: II, Grain growth in porous compacts and relation to densification, *Journal of the American Ceramics Society*, 72(5): 735-741.

Rosenthal, W., Saleta, J., and Dozier, J. (2007), Scanning electron microscopy of impurity structures in snow, *Cold Regions Science and Technology*, 47(1-2): 80-89, doi: 10.1016/j.coldregions.2006.08.006, 2007.

Schneebeli, M., and Sokratov, S. A. (2004), Tomography of temperature gradient metamorphism of snow and associated changes in heat conductivity, *Hydrological Processes*, 18(18): 3655-3665, doi: 10.1002/hyp.5800.

Szabo, D., and Schneebeli, M. (2007), Subsecond sintering of ice, *Applied Physics Letters*, 90(15): 151916, doi: 10.1063/1.2721391.